

Localized end states in density modulated quantum wires and rings

Suhas Gangadharaiah, Luka Trifunovic, and Daniel Loss

Department of Physics, University of Basel, Klingelbergstrasse 82, 4056 Basel, Switzerland

(Dated: November 4, 2018)

We study finite quantum wires and rings in the presence of a charge density wave gap induced by a periodic modulation of the chemical potential. We show that the Tamm-Shockley bound states emerging at the ends of the wire are stable against weak disorder and interactions, for discrete open chains and for continuum systems. The low-energy physics can be mapped onto the Jackiw-Rebbi equations describing massive Dirac fermions and bound end states. We treat interactions via the continuum model and show that they increase the charge gap and further localize the end states. In an Aharonov-Bohm ring with weak link, the bound states give rise to an unusual 4π -periodicity in the spectrum and persistent current as function of an external flux. The electrons placed in the two localized states on the opposite ends of the wire can interact via exchange interactions and this setup can be used as a double quantum dot hosting spin-qubits.

PACS numbers: 85.35.Be, 73.63.Nm, 03.67.Lx

Introduction. Over the last decades a number of proposals have been made for solid-state implementations of a quantum computer. Among these, electron spins in GaAs quantum dots [1, 2] are most promising candidates with unusually long coherence times [3]. Such dots contain typically many levels which are filled according to Hund's rule. Thus, the condition for a spin-qubit, which requires the presence of only a single unpaired electron, becomes challenging [2], and the scalability of such an approach is still an open problem. In this letter we propose a simple setup, involving periodically modulated gates on top of a quantum wire (see Fig. 1), which eventually results in an effective double dot system. Due to the spatial modulation of the gate voltage the energy spectrum of the quantum wire acquires a charge density wave (CDW) gap. Recently, similarly modulated setups have been discussed with focus on metal-insulator transitions [4] and transport properties in an infinite-wire superlattice [5]. Here, we show that the modulated quantum wire supports localized states at each end of the wire, known as Tamm-Shockley bound states [8, 9], with their energies lying inside the gap. These end wave-functions are well protected from the continuum and can host stable spin-qubits.

We consider one-dimensional (1D) discrete and continuum models and find a number of remarkable features for the end states resulting from the CDW modulation. In particular, using exact numerical diagonalization of the discrete open chain we analyze the stability of these states in the presence of a random potential and find that for weak disorder the end states remain stable. For the continuum model we consider a periodically modulated potential of the form $\Delta_0 \cos(k_{CDW}x + \vartheta)$, where Δ_0 is the strength of the potential, k_{CDW} the CDW vector, and ϑ a constant phase. For $\vartheta = \pi/2$, the CDW phase supports zero energy bound states which are remarkably robust to position dependent fluctuations in Δ_0 . We also show that for $\vartheta = \pi/2$ the model maps



FIG. 1. The figure shows a quantum wire (black) of length L with negatively charged gates (blue) forming a superlattice potential. Due to the induced charge density modulation a bound state at each wire end can emerge.

to the Jackiw-Rebbi model for massive Dirac fermions with midgap bound states [6]. We treat interactions via fermionic and bosonic techniques and find that they primarily renormalize the gap and decrease the localization length. We consider end states in a ring-geometry by connecting them directly via tunnel junction (see Fig. 4). The Aharonov-Bohm oscillation in such rings exhibits an unusual 4π periodicity, providing a striking signature of the existence of end states. Finally, we show that the two opposite end states serve as effective double quantum gates for spin-qubits.

Lattice model. The typical lattice model for 1D spinless fermions in the presence of CDW modulation is described by [7]

$$H = -t \sum_{j=1}^{N-1} [c_{j+1}^\dagger c_j + \text{h.c.}] + \Delta \sum_{j=1}^N \cos [2k_{CDW}ja + \vartheta] c_j^\dagger c_j, \quad (1)$$

where c_j is a fermion operator at the site j , N is the total number of lattice sites, $t > 0$ is the hopping integral, $\Delta > 0$ the CDW gap, k_{CDW} the CDW wavevector, a the lattice constant and ϑ is an arbitrary phase. The energy spectrum under the constraint of open boundary conditions is obtained by exact numerical diagonalization and we find that the criterion for the existence of bound states depends on the sign of the potential at the beginning and end sites. For illustra-

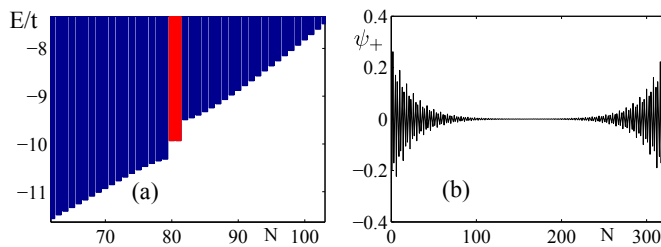


FIG. 2. (a) The part of the spectra around the gap of the Hamiltonian given by Eq. (1), obtained by exact diagonalization. The red bars denote two almost degenerate bound (midgap) states. We have chosen for the parameters $t = 7$, $\Delta = 0.8$, and $N = 320$. (b) One of two bound states. Plotted here is $\psi_+ = \psi_L + \psi_R$, where $\psi_{L,R}$ are states localized at the left (right) end of the wire.

tive purposes we have considered $k_{CDW} = \pi/4a$ and $\vartheta = \pi/2$, this choice corresponds to negative potential at the initial two sites with the overall profile given by $\Delta \sum_{j=1}^N \cos[j\pi/2 + \pi/2] \equiv \Delta(-1, 0, 1, 0, -1, \dots)$. If the phase of the potential is chosen such that one end of the wire has positive whereas the other end has negative potential then only one end state is obtained. On the other hand, for a reflection symmetric potential profile about the center of a long wire (with both ends having negative potential), there will be two degenerate mid-gap states, ψ_R and ψ_L , localized at the right and left boundaries *resp.*, being the well-known Tamm-Shockley states [8, 9]. Fig. 2(a) shows the spectrum of an 320 site chain. Reducing the wire length causes exponentially small splitting in the energies of the bound states, with the new states described by the symmetric and anti-symmetric combination of ψ_R and ψ_L . We obtain the bound states to be in the middle of the gap only when $\vartheta = \pi/2$ and $t \gg \Delta$.

Disorder effects. For realistic systems, some degree of random disorder is unavoidable. To study this effect in our lattice model, we add a random on-site potential $\sum_i V_i c_i^\dagger c_i$. Here, V_i is taken according to a Gaussian distribution with zero mean and standard deviation γ . Fig. 3 depicts the linear dependence of the root-mean-square $\sqrt{\sigma[E_i]}$ of the i -th energy level ($i = 1 \dots N$, i.e., for all energy levels) on the standard deviation of the random disorder potential [10]. Since the slopes of the bound states are less than 1, we conclude that the end states remain gapped even for disorder strengths comparable to the gap (Δ). As γ is increased, Anderson localization sets in. We also observe as γ is increased that the end states begin to mix with other (spatially) nearby localized states, thus effectively causing the end states to be more delocalized. Additionally, it is readily observed from Fig. 3 that the end states are more affected by disorder compared to all the continuum states. The ratio thereof depends on ξ/L , since this difference is coming from the spatial localization of the end states. For a

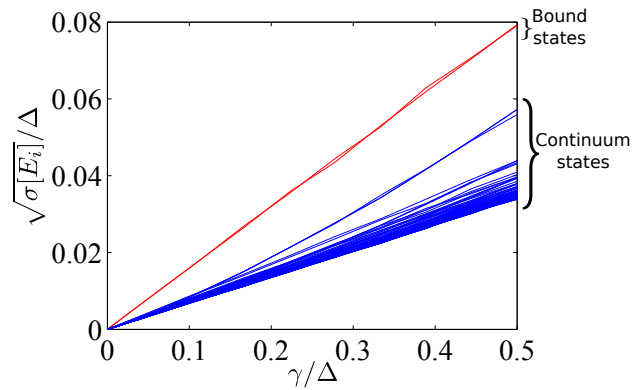


FIG. 3. The dependence of the root-mean-square value $\sqrt{\sigma[E_i]}$ of the i -th energy level ($i = 1 \dots N$, i.e., for all energy levels) on the standard deviation of the random disorder potential.

weak disorder, the aforementioned dependence is linear, while for a strong disorder the dependence becomes more complicated due to the emergence of Anderson localization.

So far we have considered a particular realization of the lattice model. We next consider the continuum case, this limit describes the low-energy physics of a large class of one-dimensional lattice models with CDW (or superlattice) modulation. Recently, there has been intense activity on exotic quantum matter, such as Majorana fermions (chargeless) [11–21] and massless Weyl fermions [22, 23] among others. Here, we will show that our setup allows for the realization of the Jackiw-Rebbi Hamiltonian [6], describing a massive Dirac fermion of charge $1/2$ as end state.

Continuum model. We consider a quantum wire in the presence of a gate-induced potential with periodicity $\lambda_{CDW} = 2\pi/k_{CDW}$. For carrier densities smaller than the intraband energy gap only the lowest subband is occupied. The physics of the fermion mode Ψ_σ ($\sigma = \uparrow, \downarrow$ is the spin index) in the lowest subband is described in terms of the slowly varying right $\mathcal{R}_\sigma(x)$ and left $\mathcal{L}_\sigma(x)$ parts and is expressed as $\Psi_\sigma(x) = \mathcal{R}_\sigma(x)e^{ik_F x} + \mathcal{L}_\sigma(x)e^{-ik_F x}$. For an open wire, the boundary condition $\Psi_\sigma(x=0) = 0$ imposes the constraint [24, 25], $\mathcal{R}_\sigma(x) = -\mathcal{L}_\sigma(-x)$. Thus, the Hamiltonian can be expressed in terms of right movers only.

The non-interacting Hamiltonian can be written as a sum of two parts, $H_0 = H_0^{(1)} + H_0^{(2)}$, where the kinetic part can be expressed in terms of only the right moving fermions (the original range $[0, L]$ now becomes $[-L, L]$) and is given by $H_0^{(1)} = -iv_F \int_{-L}^L dx \mathcal{R}_\sigma^\dagger(x) \partial_x \mathcal{R}_\sigma(x)$ (summation on the spin indices is assumed) and the CDW term by $H_0^{(2)} = \Delta_0 \int_0^L dx \cos(2k_{CDW}x + \vartheta) \Psi_\sigma^\dagger(x) \Psi_\sigma(x)$, with ϑ being a constant phase factor. Thus, $H_0 = (1/2) \int_{-L}^L dx \mathbf{R}_\sigma^\dagger \mathcal{H}_0 \mathbf{R}_\sigma$, where $\mathbf{R}_\sigma(x) =$

$[\mathcal{R}_\sigma(x), \mathcal{R}_\sigma(-x)]^T$ and the Hamiltonian density \mathcal{H}_0 for each spin is the same and given by

$$\mathcal{H}_0 = -iv_F\tau_z\partial_x + m_1(x)\tau_x + m_2(x)\tau_y, \quad (2)$$

where

$$\begin{aligned} m_1(x) &= -\cos[2\delta kx + \vartheta\text{sgn}(x)]\Delta_0/2, \\ m_2(x) &= \sin[2\delta kx + \vartheta\text{sgn}(x)]\Delta_0/2, \end{aligned} \quad (3)$$

and $\delta k = k_{CDW} - k_F$. If $\delta k = 0$ and the charge-density wave vanishes at the boundary, i.e., $\vartheta = \pi/2$, then it is easy to verify that \mathcal{H}_0 satisfies the ‘chiral symmetry’ [26] $\mathcal{P}\mathcal{H}_0 = -\mathcal{H}_0\mathcal{P}$ (\mathcal{P} is a complex conjugation operator). Moreover, the eigenvalue equation ($\mathcal{H}_0\psi_\sigma = \epsilon\psi_\sigma$) of the chiral symmetric \mathcal{H}_0 is related to the Jackiw-Rebbi equation describing massive fermions, [6, 27]

$$\mathcal{H}^{JR}\psi^{JR} = [\tau_z\partial_x + m\text{sgn}(x)]\psi^{JR} = \epsilon\tau_x\psi^{JR}, \quad (4)$$

via the transformation, $\psi^{JR} = \mathcal{U}^{-1}\tau_y\psi$ and $\mathcal{H}^{JR} = \mathcal{U}^{-1}\mathcal{H}_0\tau_y\mathcal{U}$, where $\mathcal{U} = \exp(i\vec{\tau} \cdot \hat{n}2\pi/3)$ and $\hat{n} = (\hat{i} + \hat{j} + \hat{k})/\sqrt{3}$. Here, $\tau_{x,y,z}$ denote Pauli matrices acting on the spinor $\mathbf{R}_\sigma(x)$. Solving the eigenvalue equation for $L \gg v_F/\Delta_0$ one obtains exponentially decaying bound states $\psi_\sigma \sim \exp[-(\Delta_0/2v_F)x]$ and $\psi_\sigma \sim \exp[-(\Delta_0/2v_F)(L-x)]$ at $x = 0$ and $x = L$. Away from the chiral symmetry point ($\vartheta \neq \pi/2$) bound states still exist as long as $\sin\vartheta > 0$, with the eigenstates given by $\psi_\sigma \sim \exp[-i(\Delta_0 \exp[-i\vartheta]/2v_F)x]$ and $\psi_\sigma \sim \exp[-i(\Delta_0 \exp[-i\vartheta]/2v_F)(L-x)]$. For infinite wires the eigenvalues are degenerate and given by $\epsilon = -\Delta_0 \cos(\vartheta)/2$. However, finite length introduces overlap between the end states leading to an exponentially small splitting in the energy (see below and Fig. 4).

In a realistic quantum wire the gap $\Delta(x)$ and the phase $\vartheta(x)$ will invariably be position dependent. Assuming this dependence to be weak, the correction in lowest order in $\delta(x)/\Delta_0 \ll 1$ is given by,

$$\delta\epsilon = -\frac{\Delta_0}{4v_F} \int_0^\infty dx \delta(x) \sin 2\vartheta(x) e^{-\Delta_0 \sin[\vartheta_0]x/v_F}, \quad (5)$$

where $\langle \delta(x) \rangle = 0$ and $\langle \vartheta(x) \rangle = \langle \vartheta_0 + \delta\vartheta(x) \rangle = \vartheta_0$, and they both vary slowly on the Fermi wavelength $\lambda_F = 2\pi/k_F$. Thus, $\delta\epsilon \ll \Delta_0$, and the bound states remain stable to weak perturbations.

Interaction effects. In the following, we consider the effect of repulsive interactions on the end states. For simplicity, we consider spinless fermions with $k_F = k_{CDW}$ and $\vartheta = \pi/2$. As usual in 1D, the interactions can be split into forward and back scattering parts. The former, $H_F = \pi v_F g_4 \int_0^L dx (:J_R J_R: + :J_L J_L:)$, where $J_R = \mathcal{R}^\dagger(x)\mathcal{R}(x)$ and $J_L = \mathcal{L}^\dagger(x)\mathcal{L}(x)$, is responsible for the velocity renormalization [28], $v = v_F(1 + g_4)$. On the other hand, the backscattering part, $H_B = \pi v_F g_2 \int_0^L dx :J_L J_R:$ at the lowest order in interaction renormalizes the gap. The mean-field gap $\tilde{\Delta}(x) \propto$

$g_2 v_F \langle \mathcal{R}(x)\mathcal{R}^\dagger(-x) \rangle$ adds to the externally induced gap $m_2(x) = \text{sgn}(x)\Delta_0/2$. We note that similar to $m_2(x)$, $\Delta(0_+) = -\Delta(0_-)$. This can be seen by invoking the boundary condition, $\mathcal{R}(x) = -\mathcal{L}(-x)$, and by expressing $\mathcal{R}(x) = \exp(i\sqrt{4\pi}\phi_R)$ and $\mathcal{L}(x) = \exp(-i\sqrt{4\pi}\phi_L)$ in terms of the bosonic fields $\phi_R(x)$ and $\phi_L(x)$ which themselves satisfy [24], $\sqrt{4\pi}\phi_R(0) = -\sqrt{4\pi}\phi_L(0) + \pi$. Thus, for weak interactions the bound states retain the same form as for the non-interacting case but with renormalized velocity and gap. To estimate the gap size we evaluate the self-energy, $\hat{\Sigma}$, using the unperturbed Green’s function for an infinite wire, $G_0(i\omega, k) = (i\omega - v_F k \tau_z - \Delta_0 \tau_y/2)^{-1}$. In leading order, the gap renormalizes to $(\Delta_0/2)[1 + (g_2/4) \ln[\min(\Lambda, v_F L^{-1})/\Delta_0]]$, where Λ is the band width. Thus, the localization length, given by $\xi = (2v_F/\Delta_0)\{1 + g_4 - (g_2/4) \ln[v_F/L\Delta_0]\}$, reduces with interaction. In other words, due to the repulsive interaction between the continuum and the end states, the latter states get squeezed.

The renormalization of the gap can be more rigorously analyzed via bosonization. Using standard procedures [29], we obtain the following form for the bosonic Lagrangian

$$\begin{aligned} \mathcal{L}(x, t) &= \sum_{\nu=c,s} \left[\frac{1}{2v_\nu K_\nu} (\partial_t \phi_\nu)^2 - \frac{v_\nu}{2K_\nu} (\partial_x \phi_\nu)^2 \right] \quad (6) \\ &+ \frac{v_F}{2\pi a^2} \sum_{\eta=\uparrow,\downarrow} y_\eta \sin[\sqrt{4\pi}\phi_\eta - 2\delta kx - \vartheta], \end{aligned}$$

where the subscripts c, s refer to charge and spin, *resp.* The $\partial_x \phi_{c/s}$ field describes the charge/spin density fluctuations and $\theta_{c/s}$ is the conjugated field, and $\phi_{\uparrow,\downarrow} = (\phi_c \pm \phi_s)/\sqrt{2}$. The Luttinger liquid parameters $K_{c/s}$ and velocities $v_{c/s}$ encode interactions, and $y_{\uparrow,\downarrow} = a\Delta_0/v_F$. The sine term denotes the coupling of up and down spin fermions with the external potential. As before, we assume $\delta k = 0$. In general, there are two additional terms: one of them arises due to backscattering between opposite spin electrons and is given by $\cos(\sqrt{8\pi}\phi_s)$, and the other, $\cos(4\sqrt{\pi}\phi_c - 4k_F x)$, describes the Umklapp scattering. However, both can be neglected as the two operators flow to zero under a renormalization group (RG) treatment.

The scaling dimensions of $\sin(\sqrt{4\pi}\phi_{\uparrow,\downarrow})$, $d_{\uparrow,\downarrow} = (K_c + K_s)/2 \approx 1$, indicate that near commensurability ($\delta k v_F/\Delta_0 \ll 1$) the sine terms are strongly relevant. The parameters $y_{\uparrow,\downarrow}$ have an identical flow [so as to preserve the $SU(2)$ symmetry, this also implies $K_s = 1$] towards the strong coupling regime and yields an effective localization length $\xi \sim a(a\Delta_0/v_F)^{2/(K_c-3)}$ for the bound state. Thus as before the role of the interactions is to reinforce the externally induced gap. We note that under RG additional terms of the type $\partial_i \phi_c \partial_i \phi_s$ (where $i = x, \tau$) are generated, however, they are marginal and leave the essential physics unaltered.

Detection. A viable approach for detecting the energy

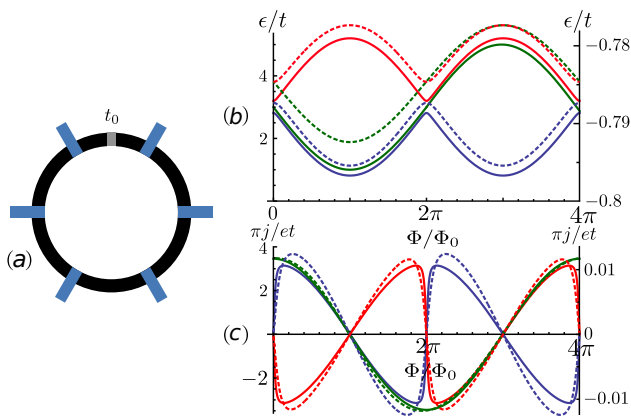


FIG. 4. (a) Quantum wire (black) in an Aharonov-Bohmring geometry with negatively charged gates (blue). The bound states are localized on either side of the weak link (grey) of strength t_0 . The energy (b) and persistent current $j = -\partial F/\partial\Phi$ (c) dependence on the flux Φ/Φ_0 are plotted with the solid curves for the effective model (Eq. (7)) and with the dashed curves for the lattice model (Eq. (1)). The parameters for the red and blue solid curves correspond to $\delta/t_0 = 2.2$ and $(\epsilon_+ + \epsilon_-)/t_0 = 6.2$, and for the green curve to $\delta/t_0 = 2.0$ and $(\epsilon_+ + \epsilon_-)/t_0 = 6.0$ (see Eq. (8)). While for the dashed curves the parameters are $\Delta/t_0 = 3.85$ (red and blue) and $\Delta/t_0 = 4.54$ (green). The ratio $\Delta/t = 0.5$ and $N = 50$ is the same for all three dashed curves. Here, t_0 is chosen such that we have a degeneracy at $\Phi/\Phi_0 = 2\pi$. Assuming only the lower bound state is filled, the persistent current shows an unusual 4π -periodicity as function of Φ/Φ_0 .

splitting between the bound states is through persistent current measurements. For this the wire should be in a ring geometry so that the end states are connected together via a tunnel junction and also large enough such that the energy splitting between the bound states is small yet the overlap of the localized wave-functions remain non-zero. Such a set-up can enclose magnetic flux Φ inducing Aharonov-Bohm (AB) oscillations in a mesoscopic (phase-coherent) regime. Next consider a single electron placed in one of the bound states. The effective Hamiltonian for the spinless fermion in terms of the orthogonal symmetric, $|+\rangle$, and anti-symmetric, $|-\rangle$, states can thus be written as [7]

$$H = \sum_{\eta=\pm} \left[\epsilon_{\eta} + \eta t_0 \cos\left(\frac{\Phi}{\Phi_0}\right) \right] |\eta\rangle\langle\eta| + it_0 \sin\left(\frac{\Phi}{\Phi_0}\right) \times \left[|-\rangle\langle+| - |+\rangle\langle-| \right], \quad (7)$$

where $\Phi_0 = h/e$ is the flux quantum, ϵ_+ (ϵ_-) the energy of the symmetric (anti-symmetric) mode, and the tunneling across the weak link is associated with a factor $\nu t_0 \exp(i\mu\Phi/\Phi_0)$, where $\nu, \mu = \pm 1$ and t_0 the tunneling amplitude. For (anti-) clockwise tunneling we have $\mu = +(-)$, while the sign of ν depends on the relative sign between the wave-functions across the weak link.

The energy eigenvalues are

$$\epsilon_{1/2} = \frac{1}{2} (\epsilon_- + \epsilon_+ \pm \sqrt{4t_0^2 + \delta^2 - 4t_0\delta \cos[\Phi/\Phi_0]}), \quad (8)$$

where $\delta = |\epsilon_+ - \epsilon_-|$. At $\Phi/\Phi_0 = 2\pi$ the separation between the two eigenvalues is minimal and given by $|2t_0 - \delta|$. For large separations, the energy levels exhibit the usual 2π dependence on the flux Φ/Φ_0 . In contrast, for a flux sweep-rate ω larger than $|2t_0 - \delta|$ a scenario emerges wherein an electron placed in one of the levels can jump to the second level and come back to the original one after a second 2π phase, thus exhibiting an unusual 4π -periodicity in the persistent current, $j = -\partial F/\partial\Phi$, where F is the free energy [30]. By independently varying t_0 and ω the splitting δ can be estimated. For typical values $t_0 \sim \delta \sim 10\mu\text{eV}$ we estimate $j \sim 0.1\text{nA}$, which is of measurable size [31, 32]. For the observation, the phase-coherence length L_{ϕ} of the ring needs to exceed L . For GaAs rings, we note that $L_{\phi} \gtrsim \mu\text{m}$ for sub-Kelvin temperatures [31, 32].

The effective model, Eq. (7), does not take into account the contribution arising from the filled Fermi sea of continuum states. However, when the number of continuum states below the gap is even—the states come in pairs with mutually canceling contributions to the current. On the other hand, when this number is odd, the topmost filled continuum state contributes to the current. Nevertheless, the amplitude of the persistent current, due to the end and continuum states, scale differently with the lattice length N —the latter behaves like $1/N$, while the former like $\delta \sim e^{-\xi/N^a}$. Thus, for chains with $N \gg 1$ and $\Delta \sim \hbar v_F/N^a$, the persistent current will be dominated by the end states and our effective description fully applies. The dashed curves in Fig. 4 include contributions from the bound states as well as the filled Fermi sea. Indeed we have confirmed that the contributions from the continuum states are two orders of magnitude less compared to those from the bound states. Finally, for the spinfull case, the amplitude of j simply doubles, whereas the periodicity remains unchanged.

Effective quantum dot. Similar to the discrete quantum dot states, the presence of spinful, CDW-induced, localized states in the quantum wire opens up an intriguing possibility for the realization of a quantum computer device. These states are well separated from the continuum and can be filled by tuning the chemical potential to the end state level. We note that these ‘quantum dots’ contain automatically only one orbital level, and no individual gates are needed to tune them into a single electron regime. Due to incomplete screening there will be half-filling, i.e., only one state on either end will be filled. This is simply because once one of the energy levels on either end is filled, to fill the remaining two levels requires additional energy to overcome the Coulomb repulsion. The physics of the half-filled state is described by the usual Hubbard model,

$H = -t \sum_{\sigma=\uparrow,\downarrow} (c_{\sigma,R}^\dagger c_{\sigma,L} + h.c.) + U \sum_{i=L,R} n_{\uparrow,i} n_{\downarrow,i}$, where t is the tunneling amplitude and U is the on-site repulsion. For the energy hierarchy $\Delta \gg U \gg t$ the effective Hamiltonian acquires the Heisenberg form, $H = J \vec{S}_R \cdot \vec{S}_L$, where $J = 4t^2/U$. The effective exchange coupling J can be controlled by changing the gate potential which determines the overlap between the left and right end modes and hence the tunneling amplitude t . We note that for weak overlap, t is small and U large making the J to be small, whereas for strong overlap the opposite is true [33]. By switching on and off the exchange constant in an appropriate sequence, the essential operations of the quantum dot, both the ‘swap’ and ‘square-root-of-swap’ operations can be performed, which, together with two single spin-qubit operations, enables the fundamental XOR gate [1].

Finite overlap between the right and the left end states can be ensured if their localization length ξ is on the order of the wire length L . This restriction yields an estimate for the strength of the periodically modulated external voltage, $\Delta_0 \sim \Lambda(a/L)^{(3-K_c)/2}$, where $\Lambda \sim v_F/a$ is the band width. A GaAs quantum wire with length $L \sim 1\mu\text{m}$ with approximately 10 – 20 gates requires a Fermi wavelength $\lambda_F \sim 50\text{nm}$. And with the parameters [34], $\Lambda \sim 0.2\text{eV}$, $K_c = 0.8$, and lattice spacing $a \approx 5\text{\AA}$, we obtain $\Delta_0 \sim 0.04\text{meV}$. Thus, the upper bound for temperatures are in the achievable range of a few hundred milli-Kelvin.

Conclusion. We have shown that a CDW gap in a quantum wire can lead to bound states at the ends of the wire which are stable against weak disorder and interactions. They map to massive Dirac fermions described by the Jackiw-Rebbi model. In an AB-ring, the bound states lead to an unusual 4π -periodicity in the persistent current. Finally, the two opposite end states serve as effective double quantum dot which can be used to implement quantum computing gates for spin-qubits.

Acknowledgements. We acknowledge discussions with K. Damle, C. Klöffel, D. Rainis, B. Röthlisberger, D. Stepanenko, and V. Tripathi. This work is supported by the Swiss NSF, NCCR Nanoscience and NCCR QSIT, DARPA, and IARPA.

[1] D. Loss and D. P. DiVincenzo, Phys. Rev. A **57**, 120 (1998).

- [2] R. Hanson *et al.*, Rev. Mod. Phys. **79**, 1455 (2007).
 [3] H. Bluhm *et al.*, Nature Physics **7**, 109 (2011).
 [4] M. Malard *et al.*, Phys. Rev. B **84**, 075466 (2011).
 [5] G. Thorgilsson *et al.*, arXiv:1111.1534 (2011).
 [6] R. Jackiw and C. Rebbi, Phys. Rev. D **13**, 3398 (1976).
 [7] For simplicity we omit here the spin indexes, since the \uparrow and \downarrow spin channels are independent and this leads only to an additional degeneracy.
 [8] I. Tamm, Phys. Z. Soviet Union **1**, 733 (1932).
 [9] W. Shockley, Phys. Rev. **56**, 317 (1939).
 [10] We note that a Kolmogorov-Smirnov test shows that the eigenenergies are not normally distributed.
 [11] A. Y. Kitaev, Phys.-Usp. **44**, 313 (2001).
 [12] O. Motrunich, K. Damle, and D. A. Huse, Phys. Rev. B **63**, 134424 (2001).
 [13] J. Sau *et al.*, Phys. Rev. B **82**, 214509 (2010).
 [14] Y. Oreg, G. Refael, and F. von Oppen, Phys. Rev. Lett. **105**, 177002 (2010).
 [15] F. Hassler *et al.*, New J. Phys. **12**, 125002 (2010).
 [16] A.C. Potter and P. A. Lee, Phys. Rev. Lett. **105**, 227003 (2010).
 [17] J. Alicea *et al.*, Nature Phys. **7**, 412 (2011).
 [18] S. Gangadharaiyah *et al.*, Phys. Rev. Lett. **107**, 036801 (2011).
 [19] M. Duckheim and P. W. Brouwer, Phys. Rev. B **83**, 054513 (2011).
 [20] E. M. Stoudenmire *et al.*, Phys. Rev. B **84**, 014503 (2011).
 [21] C. Bena, D. Sticlet, and P. Simon, arXiv:1109.5697.
 [22] X. Wan *et al.*, Phys. Rev. B **83**, 205101 (2011).
 [23] A. A. Burkov and L. Balents, Phys. Rev. Lett. **107**, 127205 (2011).
 [24] S. Eggert and I. Affleck, Phys. Rev. B **46**, 10866 (1992).
 [25] M. Fabrizio and A. Gogolin, Phys. Rev. B **51**, 17827 (1995).
 [26] A. P. Schnyder, S. Ryu, A. Furusaki, and A. W. W. Ludwig, Phys. Rev. B **78**, 195125 (2008).
 [27] The fractional charge $1/2$ of the end states are seen only in the continuum model [6] but not in the lattice model. This difference is coming from subtracting an infinite Fermi sea when passing to the continuum model.
 [28] A. O. Gogolin, A. A. Nersisyan, and A. M. Tsvelik *Bosonization and strongly correlated systems*, (University Press, Cambridge, 1998).
 [29] T. Giamarchi. *Quantum physics in one dimension*, (University Press, Oxford, 2004).
 [30] D. Loss, Phys. Rev. Lett. **69**, 343 (1992).
 [31] D. Mailly, C. Chapelier, and A. Benoit, Phys. Rev. Lett. **70**, 2020 (1993).
 [32] H. Bluhm *et al.*, Phys. Rev. Lett. **102**, 136802 (2009).
 [33] We note that because of the gap between the bound state and the continuum, Kondo physics does not play a role.
 [34] O. M. Auslaender *et al.*, Science **295**, 825 (2002).